Nonlinear Processes in Geophysics (1996) 3: 89–101

Nonlinear Processes in Geophysics

A new theoretical paradigm to describe hysteresis, discrete memory and nonlinear elastic wave propagation in rock

K. R. McCall[1] and R. A. Guyer[2]
Los Alamos National Laboratory, Los Alamos, New Mexico

[1]Present address Department of Physics, University of Nevada, Reno, Nevada
[2]Present address Department of Physics and Astronomy, University of Massachusetts, Amherst, Massachusetts

Received 15 June 1995 - Accepted 22 March 1996 - Communicated by L. A. Ostrovsky

Abstract. The velocity of sound in rock is a strong function of pressure, indicating that wave propagation in rocks is very nonlinear. The quasistatic elastic properties of rocks are hysteretic, possessing discrete memory. In this paper a new theory is developed, placing all of these properties (nonlinearity, hysteresis, and memory) on equal footing. The starting point of the new theory is closer to a microscopic description of a rock than the starting point of the traditional five-constant theory of nonlinear elasticity. However, this starting point (the number density ρ of generic mechanical elements in an abstract space) is deliberately independent of a specific microscopic model. No prejudice is imposed as to the mechanism causing nonlinear response in the microscopic mechanical elements. The new theory (1) relates suitable stress-strain measurements to the number density ρ and (2) uses the number density ρ to find the behavior of nonlinear elastic waves. Thus the new theory provides for the synthesis of the full spectrum of elastic behaviors of a rock. Early development of the new theory is sketched in this contribution.

1 Introduction

The purpose of this paper is to give an overview of a comprehensive theory of the nonlinear elastic behavior of consolidated materials. We focus on rock. This theory establishes a framework for the synthesis of static and dynamic phenomena. The central construct that makes this synthesis possible is the Preisach-Mayergoyz (P-M) space picture of the behavior of the mesoscopic mechanical elements in the rock. These mechanical elements are responsible for the macroscopic linear and nonlinear elastic behavior of the rock. In broad outline the theory uses static stress-strain data to determine the density ρ of mechanical elements in P-M space. From the density ρ the dynamic elastic response of the system is determined. The connection between static and dynamic behavior, provided by the P-M space picture, yields a qualitative and quantitative description of the relationship between the static and dynamic modulii. It yields a description of nonlinear wave propagation in qualitative and quantitative agreement with experiment.

To place this theory in context we begin in Sect. 2 with a brief sketch of the traditional (or "five constant") theory of nonlinear wave propagation and description of some of the nonlinear phenomena admitted by it. We draw attention to well known stress-strain experiments on rocks; the stress-strain equation of state has hysteresis with discrete memory. These empirical facts about the nature of rocks are at odds with the five constant theory. A theory faithful to the most rudimentary elastic properties of rocks is described in Sects. 3–5. In Sect. 3 we introduce the P-M space construct for tracking the behavior of a collection of hysteretic mechanical elements. We show that a stress-strain equation of state with hysteresis and discrete memory follows. The important physical quantity in this description of the stress-strain equation of state is ρ, the density of mechanical elements in P-M space. This density takes the place of the five constants of the traditional theory. In Sect. 4 we show how ρ is found from experiments measuring the static modulus. Finding ρ requires the solution of an ill-posed inverse problem. Using a simulated annealing procedure and static modulus data, we find ρ for a Berea sandstone. With ρ in hand, the problem of elastic wave propagation (dynamics) is straightforward. We sketch the formulation of the linear and nonlinear elastic wave propagation problem in Sect. 5. A consequence of the formulation is that the dynamic modulus is greater than or equal to the static modulus. Although most of the consequences of implementing this formulation have yet to be worked out, we give one example. For a resonant bar experiment, for which the five-constant

Correspondence to: K. R. McCall

theory is wrong both qualitatively and quantitatively, the new paradigm is in excellent agreement with experiment. The quantitative agreement results from using the P-M space density found from static measurements of the modulus, Sect. 4, illustrating the power of the new paradigm.

2 Review of the traditional theory

Rocks are consolidated materials. Their elastic properties are importantly influenced by the basic structural features in their makeup, e.g., contacts, grain boundaries, cracks, joints, and residual fluids. The extant theory of the nonlinear elastic behavior of rocks is the theory of the nonlinear elasticity of homogeneous solids. The theoretical framework that we introduce in Sect. 3 differs from this traditional theory both qualitatively and quantitatively. It predicts phenomena that are not found in the traditional theory and gives quantitatively different answers for behavior predicted by both theories. To have the basic features of the traditional theory in hand we review it here.

2.1 The five-constant theory

The traditional theory of the nonlinear elasticity of homogeneous materials is based on developing the elastic energy density as an analytic function of the strain field. This is done by constructing the scalar invariants of the strain tensor (Landau and Lifshitz, 1959; Murnaghan, 1951). Landau and Lifshitz (1959) derive the equation of motion for the displacement field $\mathbf{u}$ using

$$\begin{aligned}\mathcal{E} &= \mu\epsilon_{ik}^2 + \left(\frac{K}{2} - \frac{\mu}{3}\right)\epsilon_{ll}^2 \\ &\quad + \frac{A}{3}\epsilon_{ik}\epsilon_{il}\epsilon_{kl} + B\epsilon_{ik}^2\epsilon_{ll} + \frac{C}{3}\epsilon_{ll}^3 + \mathcal{O}(\epsilon^4), \end{aligned} \tag{1}$$

$$\sigma_{ik} = \frac{\partial \mathcal{E}}{\partial(\partial u_i/\partial x_k)}, \tag{2}$$

$$\rho_0 \frac{\partial^2 u_i}{\partial t^2} = \frac{\partial \sigma_{ik}}{\partial x_k}, \tag{3}$$

where $\mathcal{E}$ is the energy density, ρ_0 is a constant mass density, σ is the stress tensor and ϵ is the strain tensor,

$$\epsilon_{ik} = \frac{1}{2}\left(\frac{\partial u_i}{\partial x_k} + \frac{\partial u_k}{\partial x_i} + \frac{\partial u_l}{\partial x_i}\frac{\partial u_l}{\partial x_k}\right). \tag{4}$$

The constants μ, K, A, B, and C are found in principle from experiment; for example K and μ are related to the longitudinal and transverse velocities of sound. The theory embodied in Eqs. (1)–(4) is often called the five-constant theory of nonlinear elasticity.

2.2 Nonlinear phenomena

The early paper by Gol'dberg (1960) illustrates application of the Landau theory scheme to propagation of longitudinal and transverse disturbances in one direction, the x-direction, $\mathbf{u} \propto \exp ikx$. For the displacement fields in the x and y directions, u_x and u_y, Gol'dberg (1960) finds to order u^2

$$\rho_0 \ddot{u}_x - \alpha u_x'' = S_x + \beta u_x' u_x'' + \gamma u_y' u_y'', \tag{5}$$

and

$$\rho_0 \ddot{u}_y - \mu u_y'' = S_y + \gamma u_x' u_y'' + \gamma u_y' u_x''. \tag{6}$$

where $\partial u/\partial t = \dot{u}$, $\partial u/\partial x = u'$, S_x and S_y are the sources of longitudinal and transverse distrubances, and the constants α, β and γ are linear combinations of K, μ, A, B and C

$$\alpha = K + \frac{4}{3}\mu, \tag{7}$$

$$\beta = \alpha + 2A + 6B + 2C, \tag{8}$$

$$\gamma = \alpha + \frac{A}{2} + B \tag{9}$$

Equations (5) and (6) admit a variety of nonlinear processes.

1. $(S_x \neq 0, S_y = 0)$ A longitudinal wave is launched that in second order (i.e., the term $\beta u_x' u_x''$ in the u_x equation) coalesces to produce longitudinal waves at frequencies $\omega+\omega = 2\omega$ and $\omega-\omega = 0$. This is an $l + l \rightarrow l$ process, where l stands for a longitudinal wave.

2. $(S_x = 0, S_y \neq 0)$ A transverse wave is launched that in second order (due to $\gamma u_y' u_y''$ in the u_x equation) coalesces to produce a longitudinal wave. This is a $t + t \rightarrow l$ process, where t stands for a transverse wave. There is no $t + t \rightarrow t$ process.

3. $(S_x \neq 0, S_y \neq 0)$ A longitudinal wave and a transverse wave are launched that in second order (due to $\gamma(u_x' u_y'' + u_y' u_x'')$ in the u_y equation) coalesce to produce a transverse wave. This is an $l + t \rightarrow t$ process.

4. S_x may produce a static distortion, a constant value of u_x, that modifies the sound velocity for a longitudinal wave. A scheme to measure A, B and C can be developed using this coupling. Similar observations apply to application of a constant torque.

Items 1–4 are a few of the consequences of nonlinearity; they are the physical events behind strong ground motion, bent tuning-fork curves, etc. A systematic treatment of the problem set by equations like Eqs. (5) and (6) has been given by McCall (1994), using a Green function procedure. This treatment lets one picture the

physical processes that occur in the rock and see the involvement of the physical parameters, e.g., the strength of the strain, A/α, B/α, and C/α. This treatment is accompanied by a language that facilitates the description of nonlinear phenomena and has commonality with the description of similar processes in other contexts. The α and μ terms in the equations of motion, coming from terms in the energy that are quadratic in u, are the harmonic terms. The terms in the energy that are cubic and quartic in u are called the cubic and quartic anharmonicities. The cubic anharmonicity is responsible for the 3-wave processes, items 1–3 above.

The equations investigated by Gol'dberg (1960) include only cubic anharmonicity. An exhaustive description of the possible three-wave processes permitted by cubic anharmonicity has been given by Jones and Kobett (1963). The static/dynamic couplings described under item 4 are 3-wave processes in which one of the waves is a static wave with wavevector $k \to 0$. A description of the coupling of acoustic waves to static displacement fields has been given by Johnson and Rasolofosaon (1993). The nonlinear coefficients A, B and C have recently been measured for a Berea sandstone in experiments in which a sound wave was coupled to static displacement fields (Johnson et al., 1994). The traditional theory, in which the stress is taken to be an analytic function of the strain, has been very successful in describing wave propagation in many homogeneous materials (Ashcroft and Mermin, 1976; Ilinskii and Zabolotskaya, 1992).

2.3 Order of magnitude

The orders of magnitude of the harmonic elastic constants α and μ (or K and μ) are found from the velocities of sound. In a typical rock at atmospheric pressure

$$c_0^2 \approx (2000\text{m/s})^2 \approx \frac{\alpha}{\rho_0}, \tag{10}$$

where c_0 is the compressional velocity. Using $\rho_0 \approx 2$–4 gm/cm^3, $\alpha \approx \mu \approx K \approx 10^{11}$ dyne/cm$^2 \approx 10000$ MPa. Estimates of the order of magnitude of the cubic and quartic anharmonicity come from writing

$$c^2 \approx c_0^2 \left[1 + \beta(\nabla \cdot \mathbf{u}) + \delta(\nabla \cdot \mathbf{u})^2\right]. \tag{11}$$

At a pressure of order 100 MPa the velocity of sound of a typical rock (see chapter 10 of Bourbie et al. (1987)) has saturated at about twice the atmospheric pressure value. Using $\Delta P \approx -K\nabla \cdot \mathbf{u}$, Eq. (11) becomes

$$c^2 \approx c_0^2 \left[1 - \beta\frac{\Delta P}{K} + +\delta\left(\frac{\Delta P}{K}\right)^2\right]. \tag{12}$$

Ignoring the quartic anharmonicity for the moment, the requirement that $c^2 \approx 2c_0^2$ when $\Delta P/K \approx 0.01$ gives $-\beta\Delta P/K \approx 1$ or $\beta \approx -100$. Retaining the quartic term and requiring c^2 to saturate at $\Delta P/K \approx 0.01$ means $c^2(2[0.01]) \approx 2c_0^2$,

$$-\beta\frac{2\Delta P}{K} \approx \delta(\frac{2\Delta P}{K})^2 \approx 1, \tag{13}$$

and $\delta \approx -\beta^2 \approx -10^4$. These estimates are very crude but they point to the fact that A/α, B/α, and C/α for rock are large compared to 1 and large compared to A/α, B/α and C/α for normal materials. It must be emphasized that the size of these dimensionless measures of nonlinearity does not invalidate the analytic expansion. These coefficients, large compared to 1, are multiplied by powers of the strain. The proper dimensionless measures of the importance of various nonlinear terms are $\beta(\nabla \cdot \mathbf{u})$, $\delta(\nabla \cdot \mathbf{u})^2$, etc.

2.4 Experiment

When the nonlinear coefficients A, B and C are measured for rocks they are found to be several orders of magnitude greater than for Al, H_2O, etc. Nonetheless Eqs. (1)–(4) are used for rocks. That is, rocks are assumed to be homogeneous materials that do not differ from Al qualitatively but only quantitatively. The physical mechanism of nonlinearity in normal materials is an anharmonic interaction of microscopic origin. It is due for example to the shape of the interatomic van der Waal forces. However the fact $A_{\text{rock}} >> A_{\text{Al}}$ does not mean that the interatomic force in rock is orders of magnitude different from that in Al. It means that the source of the important elasticity in rock is in mechanical elements different in character from those in Al. These elements are the structural features in the rock, typically of size 1 μm, i.e., mesoscopic. Their mechanical behavior masks the underlying elastic behavior due to the atomic scale forces. If we use the traditional theory it is equivalent to saying that these very different mechanical elements are nonetheless at most quantitatively different from the elastic elements in homogeneous materials. They are not qualitatively different. To the contrary, experimental evidence gives us reason to believe that this is not true.

The results of experimental measurements present a number of puzzles for which the traditional theory provides no ready explanation. For example, the traditional theory is unable to explain the relationship between modulus measured dynamically and modulus measured statically. But even before the five-constant theory is applied to the dynamic/static puzzle there is something amiss. Rocks have a stress-strain equation of state with hysteresis and discrete memory (Holcomb, 1981; Gist, 1994; Scholz and Hickman, 1983). In rock the stress is not an analytic function of the strain. Neither is the energy density. This simplest of observations is at odds with the basic starting point of the traditional theory, Eq. (1).

An explanation for why a theoretical model strikingly at odds with empirical facts has been employed, consists of arguing that: a) nonlinear effects are small, so precise treatment is not necessary, and b) hysteresis is a nuisance to be ignored or possibly removed by suitable cycling of the sample. Intensified experimental interest in

nonlinearity in rocks (Meegan et al., 1993; Johnson and McCall, 1994) and the realization that nonlinear effects are not modest in several important circumstances (e.g., strong motion, near source region propagation, resonant bar behavior) require us to do better. There is need for a theoretical framework that is faithful to the nature of rock and capable of qualitative and quantitative description of rock properties.

3 The new paradigm

The elastic properties of a rock are determined by the principal mechanical elements of which it is composed. These mechanical elements are the structural features in the interior of the rock, the medley of inhomogeneities remarked on above. They are a complicated set of objects, each a structural anecdote with properties specific to its details. We proceed by a method that avoids adopting a detailed model for these structural features, e.g., cracks (O'Connell and Budiansky, 1978; Cheng and Toksöz, 1979), friction between surfaces (Hilbert et al., 1994). However, we cannot altogether avoid assigning properties to the mechanical elements, e.g., a spring constant, or an equilibrium length. We adopt a minimalist point of view and assign to each mechanical element no more characterizing properties than are necessary to meet data. One of the virtues of the new paradigm is that it provides a recipe for extracting the properties assigned to the mechanical elements from experiment.

3.1 The ingredients

The elastic properties of a rock are due to an assembly of mechanical elements. To calculate the elastic properties of the rock from the properties of the mechanical elements we need several ingredients.

1. Represent the elastic properties of the rock by the elastic properties of a lattice of mechanical elements. The mechanical elements are structural features of typical size 1μm. Thus the lattice spacing between mechanical elements is neither microscopic (10^{-8} cm), nor macroscopic (1 cm). The mechanical elements and the lattice on which they reside involve mesoscopic length scales.
2. Model the mechanical elements with a hysteretic set of springs.
3. Prescribe the pressure protocol by which the current state of the rock was obtained.
4. Prescribe an assembly procedure. That is, a computational procedure for turning 1–3 into an equation of state, e.g., effective medium theory (EMT) or numerical integration.

Item 3 has special importance. Rocks are made up of mechanical elements of such complexity that there is no single answer to "what is the velocity of sound in Berea sandstone at 10 MPa?" The answer to this question depends on how the rock got to 10 MPa. Rocks are made up of mechanical elements whose properties depend upon how they got to their current pressure. Thus the nature of the mechanical elements confers special status on the pressure protocol. A theory that does not give the pressure protocol this status cannot be right.

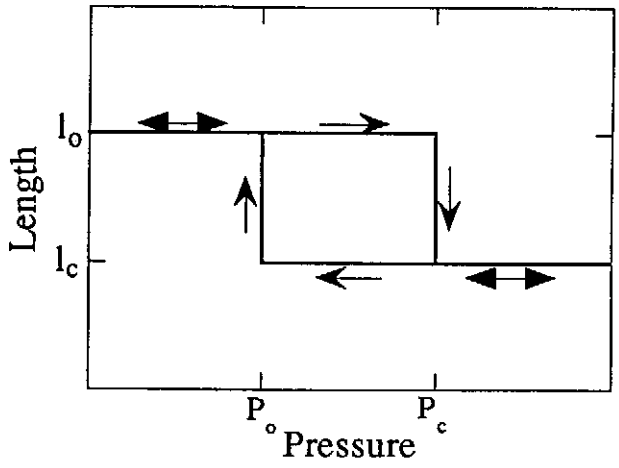

Fig. 1. Rudimentary elastic unit. The elastic properties of the macroscopic system are due to an ensemble of hysteretic mesoscopic units. A unit is modeled as having an equilibrium length that switches between two states hysteretically.

As we proceed we will put aside for the moment discussion of attenuation, the influence of pore fluids, etc. These important features can be added in a natural way once the basic ideas are in hand.

3.2 The elastic elements

A central construct, Preisach-Mayergoyz space, is introduced as a device to keep track of the state of the mechanical elements (Preisach, 1935; Mayergoyz, 1985). We adopt a simple model for the mechanical elements, taking them to be springs (see Fig. 1) that enforce two equilibrium lengths, l_c and l_o, according to the pressure. Thus a given mechanical element is characterized by two pairs of numbers, (l_c, l_o) and (P_c, P_o). Here P_c (P_o) is the pressure at which the mechanical element switches from enforcing the longer length (shorter length), l_o (l_c), to enforcing the shorter length (longer length), l_c (l_o), as the pressure is increased (decreased). This choice for the behavior of the mechanical elements will let us illustrate matters of principle with a minimum of mathematical complication. Further, this choice is suggested by the empirical fact about the σ-ϵ relation in rock that upon pressure reversal the strain stays in.

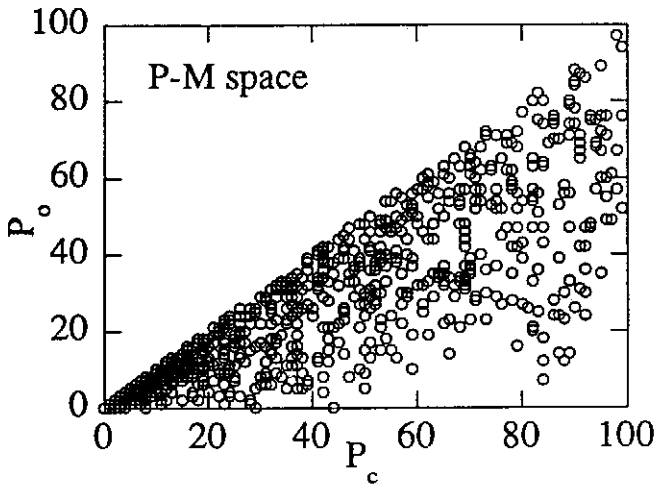

Fig. 2. Preisach-Mayergoyz space (P-M space). The mechanical elements have hysteretic properties characterized by the pressure pair (P_c, P_o). For each mechanical element in the system the point (P_c, P_o) is plotted in P_c-P_o space. The density of points is represented by $\rho(P_c, P_o)$. Here 1000 points generated by Eqs. (15) and (16) are shown. This density is used in the majority of calculations in Sect. 3.

3.3 Preisach-Mayergoyz (P-M) space

The rock is made up of mechanical elements (Fig. 1) with a spectrum of the basic properties, i.e., each element is described by two pairs (l_c, l_o) and (P_c, P_o). A further simplification is made by taking l_c and l_o to be the same for all mechanical elements. Then the mechanical elements differ from one another only because of the pressure pair (P_c, P_o) at which they respond. To track the behavior of the mechanical elements, we plot the point (P_c, P_o) for each element in P_c-P_o space or Preisach-Mayergoyz (P-M) space. A point on the diagonal, at $P_c = P_o$, corresponds to a mechanical element that closes and opens at the same pressure. This mechanical element is not hysteretic, although it behaves differently at low pressure, where it enforces l_o, than at high pressure, where it enforces l_c. In Fig. 2 we show an example of P-M space constructed by the rule given in Eqs. (15)–(16) below.

3.4 The pressure protocol

Let us follow the mechanical elements through an example pressure protocol, shown in Fig. 3a. In Table 1 we list several points on the pressure protocol and indicate the portion of P-M space in which the mechanical elements are closed (the separation l_c is enforced). For example at point A the mechanical elements in the triangle OAH of Fig. 3b are closed (P exceeds P_c for these elements). Further increase of the pressure to B closes the mechanical elements in $HABG$. The pressure reversal at B, back to A' in Fig. 3a, re-opens (the separation l_o is enforced) the mechanical elements in the triangle ABZ, where Z is the point of intersection of AE and BG. As

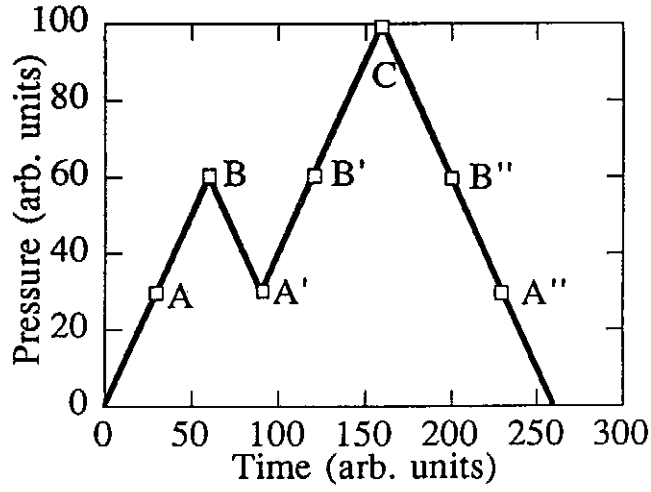

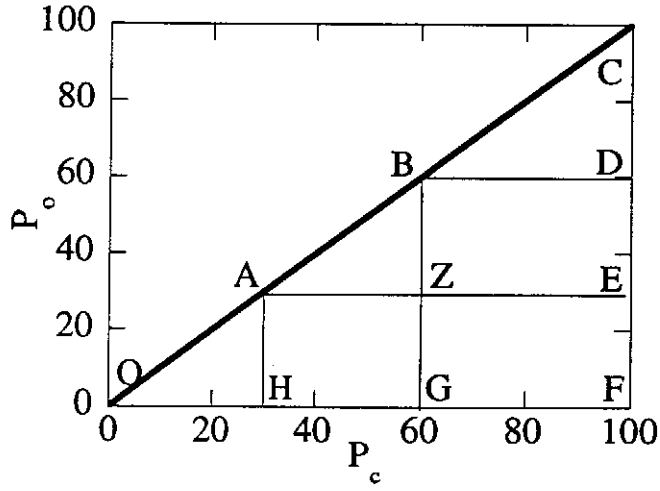

Fig. 3. Pressure protocol and P-M space. (a) The pressure protocol, P as a function of time. The mechanical elements that are in their closed configuration can be tracked in (b) P-M space. As this pressure protocol is followed, the area of P-M space in which the mechanical elements are in their closed configuration is shown in Table 1.

the pressure is increased from A to B the mechanical elements in $ABGH$ change state. Upon pressure reversal, from B to A', only the mechanical units in ABZ return to their original state. Thus there is hysteresis in the number of open and closed mechanical elements. This hysteresis is the source of the macroscopic hysteresis of the rock. One can follow pressure protocols that include interior loops or nested interior loops and show that discrete memory (end point memory) is a result of using the P-M space picture.

The P-M space picture we are developing treats the individual mechanical elements as independent. Each sees the external pressure and responds to it. This is an approximation to the truth. The random arrangements of mechanical elements in the rock will cause the rock to carry the pressure inhomogeneously; some mechanical elements will have to support more (less) than the

Table 1. Pressure vs P-M space configuration. The pressure points in Fig. 3a are listed in column 1. In column 2 the part of P-M space with closed elastic elements is indicated, Fig. 3b.

Pressure Point	Closed Area
A	OAHO
B	OBGO
A'	OAZGO
B'	OBGO
C	OCF
B"	OBDFO
A"	OAEFO

average pressure. An experimental test can be made to test the validity of the P-M space independent element approximation. The two pressure protocols in Fig. 4a should produce the same σ-ϵ hysteresis loop provided there is no interaction between the mechanical elements in $CDEF$ and those in 123 in Fig. 4b. With the first pressure protocol the mechanical elements in $CDEF$ are in their open configuration as the pressure cycle 123 takes place. With the second pressure protocol the mechanical elements in $CDEF$ are in their closed configuration as the pressure cycle 123 takes place. If the two hysteresis loops are congruent the state of the mechanical elements in $CDEF$ has not influenced the mechanical elements that respond to the 123 pressure cycle.

This example demonstration of hysteresis and discrete memory is independent of the procedure for finding the macroscopic elasticity from the collection of mechanical elements. Hysteresis and discrete memory are inherent in the behavior of the mechanical elements to be assembled. The precise rule of assembly, e.g., effective medium theory (EMT), does not effect the outcome.

3.5 Calculations of σ-ϵ

To calculate an example stress-strain relation we take the following steps.

1. Take the lattice of mechanical elements to be a one dimensional array of N elements, $i = 1, \ldots, N$.

2. Assign the same set of lengths to each mechanical element,

$$l_o = 1.0, \quad l_c = 0.9 \quad \forall i. \tag{14}$$

The strain field is our goal, thus the relevant quantity is $(l_o - l_c)/l_o$ and it is unnecessary to specify the units of length. Microns would be sensible units.

3. Distribute the pairs (P_c, P_o) according to

$$p(P_c) = 100 r_c^2, \tag{15}$$

$$p(P_o) = p(P_c)\sqrt{r_o}, \tag{16}$$

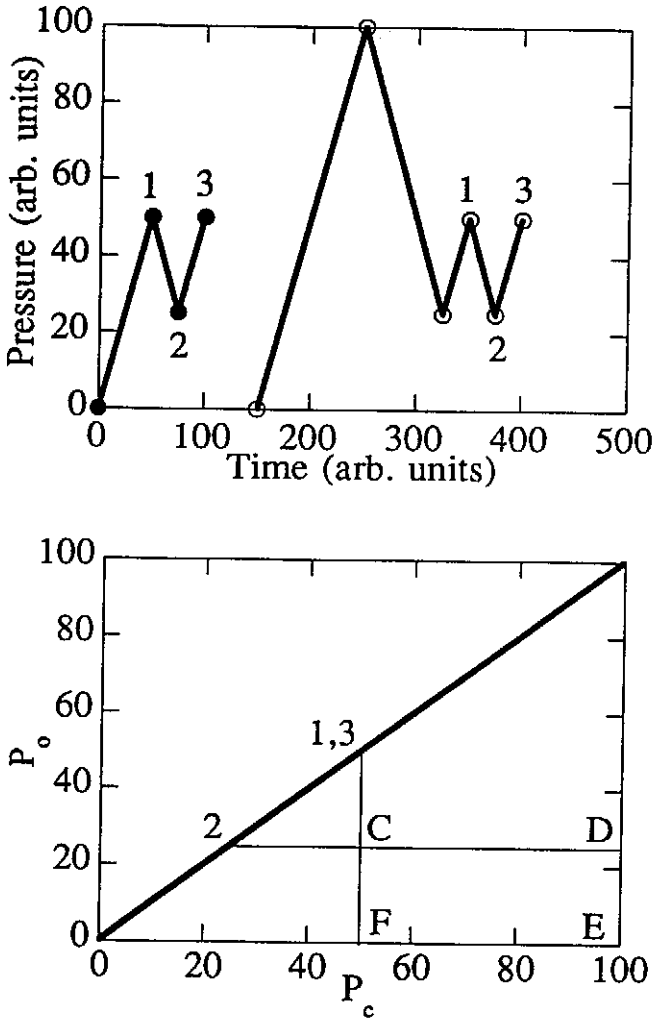

Fig. 4. Congruence and independence. (a) Two pressure protocols are shown that lead to a closed cycle $1 \rightarrow 2 \rightarrow 3$. These pressure protocols differ in terms of the configuration of mechanical elements in P-M space, (b). In the first protocol the mechanical elements in $CDEF$ are open; in the second protocol they are closed. If the stress-strain loop associated with the cycle $1 \rightarrow 2 \rightarrow 3$ is the same for both protocols then the mechanical elements in $CDEF$ do not interact with the mechanical elements in 123. This is an example of an empirical test of the validity of the simple picture we are using.

where $p(P)$ is the probability of the occurrence of P, and r_c and r_o are random numbers distributed uniformly between 0 and 1.

4. Use the pressure protocol shown in Fig. 3a.

From 1 and 2 it follows that the length of the sample is

$$L = N[0.9f + 1.0(1-f)], \tag{17}$$

where f is the closed fraction of the mechanical elements. The fraction f is a function of the pressure protocol. The L-f relationship is directly related to the L-P relationship; it is the elastic equation of state. In Fig. 5a we show the σ-ϵ relation, $[L(P) - L(0)]/L(0)$ vs P, for the pressure protocol in Fig. 3a. At $P = 0$, $f = 0$, and $L(0) = Nl_o$. Note the hysteresis and end point memory. The σ-ϵ equation of state in Fig. 5a is found from following the pressure numerically through the P-M space of Fig. 2 with $N = 8000$.

3.6 The modulus

Given the stress-strain relation, we can study the elastic modulus. The stress-strain relation is hysteretic with end point memory. Thus we need a definition of the modulus that respects these properties and is consistent with experiment. A σ-ϵ equation of state results from a quasistatic measurement. We will refer to such a measurement as static and the modulus derived from such a measurement as the static modulus. The static modulus is a measure of the pressure response of the system and we define it as follows.

1. If the pressure is being increased, $P \to P + \Delta P$,

$$\frac{1}{K} = -\frac{1}{L(P)}\frac{L(P+\Delta P) - L(P)}{\Delta P}. \tag{18}$$

2. If the pressure is being decreased $P \to P - \Delta P$,

$$\frac{1}{K} = -\frac{1}{L(P)}\frac{L(P) - L(P-\Delta P)}{-\Delta P}. \tag{19}$$

This definition is given in terms of the inverse of the modulus for later convenience. It is designed so that it does not involve pressure reversal.
An illustration of the modulus calculated in this way is given in Fig. 5b. The stress-strain curves from which the modulus is calculated are shown in Fig. 5a. The static modulus has a bowtie-like shape. At the points of pressure reversal it is discontinuous. The static modulus satisfies the equation

$$\oint d\epsilon K = 0, \tag{20}$$

where the integral is around a pressure protocol from an initial configuration and returning in P-M space to that configuration.

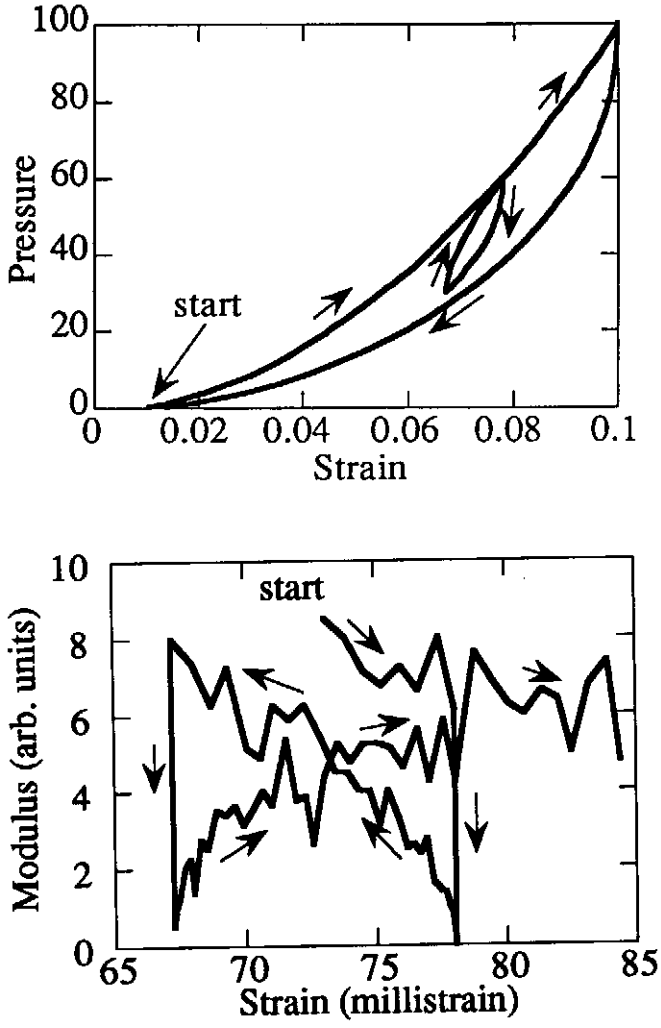

Fig. 5. Equations of state. (a) The stress-strain equation of state for the the P-M space density shown in Fig. 2 and the pressure protocol shown in Fig. 6a. This equation of state was calculated using using Eq. (17) and $\epsilon = (L(P) - L(0))/L(0)$. (b) The static modulus as a function of strain corresponding to (a). The modulus is shown for the strain interval near the interior loop corresponding to the pressure cycle 60 → 30 → 60. This is equivalent to a strain loop 0.0787 → 0.067 → 0.078. Note the bowtie character of the behavior of the modulus as this loop is traversed.

In Sect. 5 we develop this scheme further to discuss the dynamic response of the rock. Before we turn to dynamics we discuss the determination of the contents of P-M space. As P-M space is the central construct from which the elastic properties of the rock are found we want to do better than guess $\rho(P_c, P_o)$.

4 The new paradigm backward

The central construct from which the static properties of the rock are determined is P-M space. Using the P-M space picture we found the σ-ϵ equation of state and the static modulus. This forward modeling was easy because we chose an arbitrary density $\rho(P_c, P_o)$ of mechanical elements in P-M space, Eqs. (15)–(16). There are a couple of ways in which we might find a more suitable $\rho(P_c, P_o)$. One procedure is to decide upon a model for the structural features of importance and to develop its consequences. The work of O'Connell and Budiansky (1978) and Cheng and Toksöz (1979) typifies this approach. A second procedure is to try to extract suitable information from experiment. That is, to attempt to solve an inverse problem. Given some σ-ϵ data, what are the properties of the mechanical elements responsible for it? Here we discuss this inverse problem.

4.1 $\rho(P_c, P_o)$ from the static modulus

The relationship between $\rho(P_c, P_o)$ and the static modulus depends upon the ingredients to be assembled and the assembly procedure. In Sect. 3.4 we chose particularly simple properties for the ingredients. This choice led to the equation of state, Eq. (17), and will let us explore the K-ρ relation explicitly. Combining the definition of the modulus, Eqs. (18)–(19), with the equation of state, Eq. (17), we have

$$\frac{1}{K} = \frac{\Delta\epsilon}{\Delta P}\left[f(P+\Delta P) - f(P)\right], \tag{21}$$

when the pressure is being increased, and

$$\frac{1}{K} = \frac{\Delta\epsilon}{\Delta P}\left[f(P) - f(P-\Delta P)\right]. \tag{22}$$

when the pressure is being decreased. The change in strain $\Delta\epsilon \approx (l_o - l_c)/l_o$. Note that $f(P+\Delta P) - f(P)$ in Eq. (21) is related to a column region in P-M space (see Fig. 6) and $f(P) - f(P-\Delta P)$ in Eq. (22) is related to a row region in P-M space. As the two pressure points are brought close together, i.e., as ΔP is decreased, the measurements of K become measures of narrow strips of the density in P-M space. Elaborate pressure protocols permit examination of very particular collections of mechanical elements (see the discussion involving Fig. 4).

4.2 Implementation

A procedure suggested by Eqs. (21)–(22) has been implemented by Guyer et al. (1995) as described below.

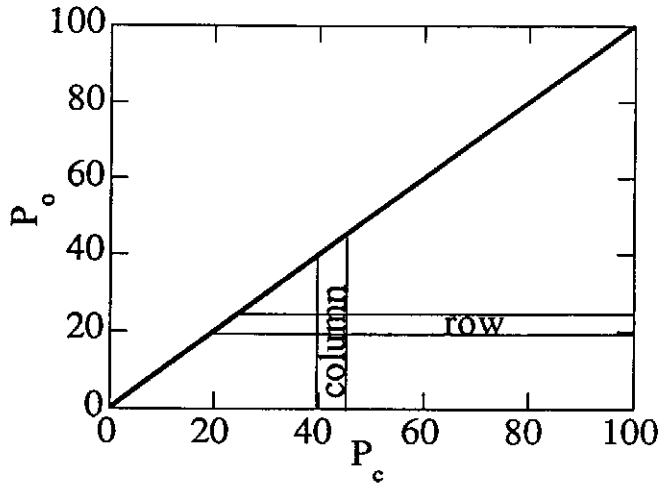

Fig. 6. P-M space and the modulus. The static modulus is related to the change in the strain accompanying a small pressure change. Small changes in pressure bring about the participation of additional mechanical elements in a column (if the pressure is being increased) or a row (if the presure is being decreased). This leads to the possibility of relating row and column sums to the inverse modulus. See Eqs. (23) and (24).

1. The σ-ϵ data, shown in Fig. 7, was taken on a Berea sandstone using the pressure protocol shown in the inset of Fig. 8 (Boitnott, 1993).

2. For the largest pressure loop, the primary loop, the pressure protocol is 0.7 MPa $\rightarrow$ 13.5 MPa $\rightarrow$ 0.7 MPa. The 2280 measured (P, ϵ) pairs on the primary loop (Fig. 8) were smoothed and used to construct a K-P curve with 60 pairs (K, P), 30 values of K for pressure increase and 30 values of K for pressure decrease.

3. A P-M space with $0.7 \leq P_c, P_o \leq 13.6$ MPa was ruled into 30×30 boxes, at $(P_c, P_o) = (m\Delta P, n\Delta P)$, where $\Delta P = 0.12$ MPa, and m and n are integers from 1 to 30.

4. From Eq. (21) we have

$$\frac{1}{K_m} = \frac{1}{K(P_m)} = \frac{\Delta\epsilon}{\Delta P}\sum_{j=1}^{m}\rho(m, j), \tag{23}$$

where $P_m = m\Delta P$. From Eq. (22) we have

$$\frac{1}{K_n} = \frac{1}{K(P_n)} = \frac{\Delta\epsilon}{\Delta P}\sum_{i=n}^{30}\rho(i, n) \tag{24}$$

where $P_n = n\Delta P$, $1 \leq m \leq 30$, $1 \leq n \leq 30$ and $\rho(m, n)$ is the number of mechanical units in the box at $(P_c, P_o) = (m\Delta P, n\Delta P)$.

5. Equations (23)–(24) are 60 equations for $30\times(30+1)/2 = 465$ numbers. The inversion for $\rho(m, n)$ is highly underconstrained. A simulated annealing

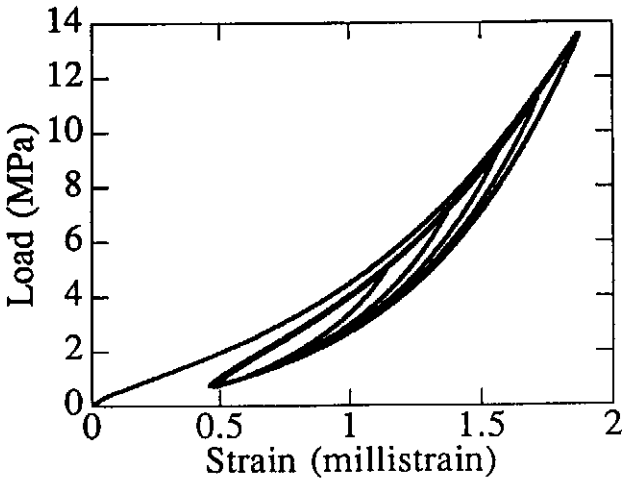

Fig. 7. Stress-strain data on Berea sandstone. Stress is plotted as a function of strain for the pressure protocol shown in the inset in Fig. 8. Details of the experiment from which these data are taken are found in Boitnott (1993).

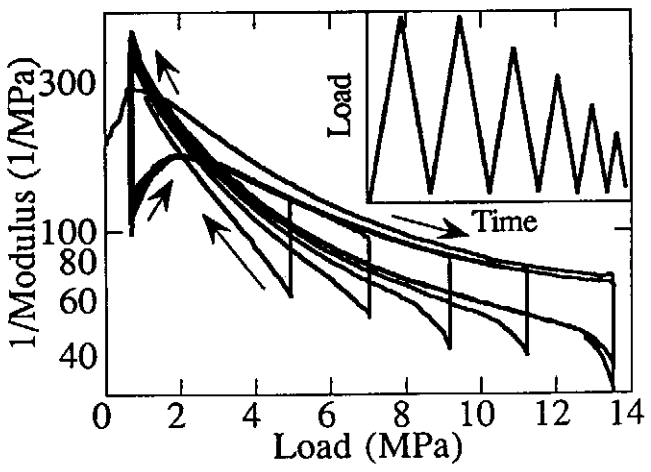

Fig. 8. Inverse modulus vs pressure. The inverse modulus, calculated according to Eqs. (18) and (19), for the stress strain data in Fig. 7. The insert shows the pressure protocol used in taking the data in Fig. 7.

procedure was used to find the 465 numbers $\rho(m,n)$ (Press et al., 1986).

Details of carrying out the calculation described here are found in the paper by Guyer et al. (1995). The results of that calculation are shown as the P-M space density in Fig. 9. Roughly 50% of the mechanical units are on the diagonal within our ability to resolve it, i.e., the limit set by $\Delta P = 0.12$ MPa. The density falls off rapidly as (P_c, P_o) moves away from the diagonal. This fall off is least rapid at low pressure. The majority of the hysteretic mechanical elements respond at low pressures. We can test the adequacy of this determination of $\rho(P_c, P_o)$ by looking at pressure protocols different from the primary pressure protocol that was used to learn $\rho(P_c, P_o)$. The experiment that carried the rock through the primary protocol also carried it through 4 smaller, closed pressure loops. The modulus from these loops was calculated from the experimental data as described in 1 and 2 above. It was also calculated using the scheme of Sect. 3, Eqs. (18)–(19), and the $\rho(P_c, P_o)$ in Fig. 9. Comparison of the experimental and theoretical determination of the modulus for these loops is shown in Fig. 10. The agreement is gratifying.

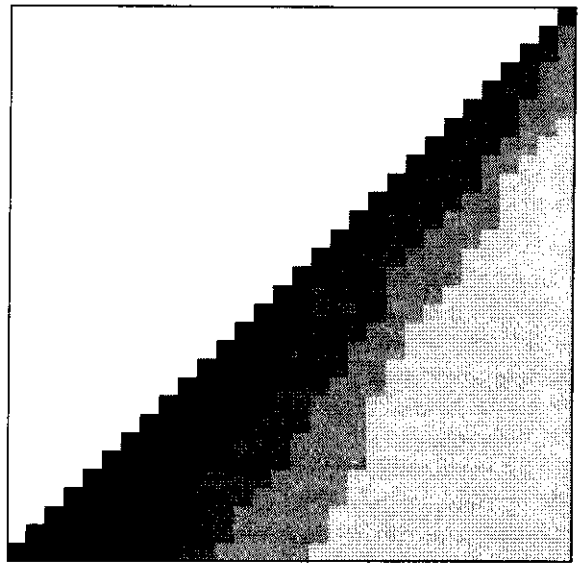

Fig. 9. P-M space density. The density of mechanical units in P-M space is shown for the analysis of the inverse modulus-pressure data of Fig. 8 using the scheme described in Sect. 4. The gray scale is logarithmic.

5 Dynamics

In Sect. 3 we used the P-M space picture to describe and understand the static behavior of a rock. We showed how to use experimental data to learn the contents of P-M space, $\rho(P_c, P_o)$, in Sect. 4. Here we turn to the use of the P-M space picture to describe the response of a rock to dynamic disturbances, i.e., to the propagation of sound waves. We adopt the view that a sound wave propagating in a material carries the material through

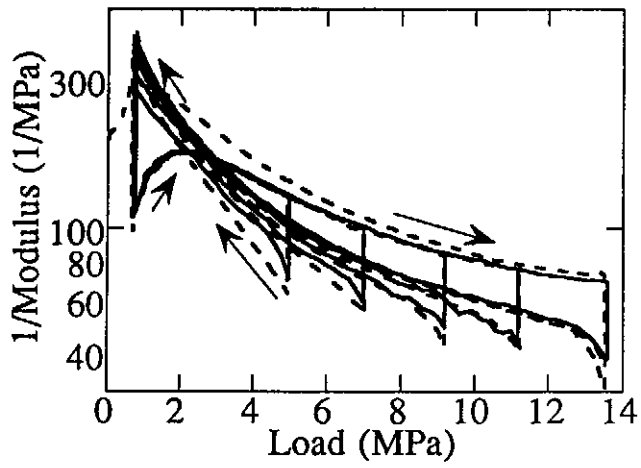

Fig. 10. Inverse modulus vs pressure. The dashed curve is the same as the solid curve in Fig. 8, the inverse modulus found from the σ-ϵ data in Fig. 7. The solid curve shows calculation of the inverse modulus from the P-M space density determined using the largest stress-strain loop in the data of Fig. 7 and the procedure described in Sect. 4. In the experiment the largest pressure loop was traversed twice (see the pressure protocol in Fig. 8 inset); the P-M space density was found using the inverse modulus from the second traversal. See Guyer et al. (1995) for details.

a sinusoidal pressure fluctuation, i.e., a sinusoidal pressure protocol of modest amplitude. The rock is brought to an elastic state, characterized by $\overline{P}$, by a quasistatic pressure protocol. In this state it is subject to a sinusoidal pressure disturbance, a sound wave.

5.1 Sound waves

To describe a sound wave in a rock we take the equation of motion of the displacement field $\mathbf{u}$ to be

$$\rho_0 \frac{\partial^2 u}{\partial t^2} = \frac{\partial}{\partial x}\left(K[\delta P]\frac{\partial u}{\partial x}\right), \tag{25}$$

where for illustrative purposes we consider propagation of a longitudinal disturbance in the x direction, $\mathbf{u} = (u, 0, 0)$. The elastic modulus in this equation is a functional of the pressure excursion δP, and the density ρ_0 is taken to be constant. We develop a model for K based on the model of the static response developed above. To do this we need the density of mechanical units in P-M space. As the pressure disturbance caused by a sound wave is modest we only need the density $\rho(P_c, P_o)$ near the diagonal, i.e. $P_c \approx P_o$. We assume that near the diagonal $\rho(P_c, P_o)$ is of the form

$$\rho(P_c, P_o) = A(P)\delta(P_c - P_o) + \rho_B, \tag{26}$$

where $A(P)\delta(P_c - P_o)$ describes the mechanical elements in ρ that have no hysteresis (the elements on the diagonal in P-M space), and ρ_B, a constant, describes the hysteretic mechanical elements (the background density near the diagonal in P-M space).

We take A to depend on pressure P, where $P = P_c$ for decreases in pressure and $P = P_o$ for increases in pressure (see below). The uniform background could also depend upon P_c and P_o but already with this form the model is flexible enough to describe most experiments. Equation (26) is consistent with the empirical P-M space in Fig. 10. Choosing $P = \overline{P} + p$, where $-\Delta P \le p \le \Delta P$, we expand the diagonal part of the density in p around $\overline{P}$,

$$\rho(P_c, P_o) = \left[a_0 + a_1 p + a_2 \frac{p^2}{2} + \cdots\right]\delta(P_o - P_c) + \rho_B. \tag{27}$$

We use $\rho(P_c, P_o)$ to find the elastic modulus as the rock is carried through the sinusoidal pressure protocol $\overline{P} + \Delta P \rightarrow \overline{P} - \Delta P \rightarrow \overline{P} + \Delta P$, where $\overline{P}$ characterizes the quasistatic state of the rock before the sound wave of amplitude ΔP is turned on. From Eqs. (21)–(22) we find the modulus

$$\frac{1}{K} = \Delta\epsilon \frac{df}{dP}. \tag{28}$$

The fraction of elements closed f depends on whether pressure is decreasing or increasing. As the pressure decreases $\overline{P} + \Delta P \rightarrow \overline{P} - \Delta P$,

$$f_\downarrow(\overline{P} + p) = f(\overline{P} + \Delta P) + \int_{\overline{P}+\Delta P}^{\overline{P}+p} dP_o \int_{P_o}^{\overline{P}+\Delta P} dP_c \cdot \left[A(\overline{P} + p')\delta(P_c - P_o) + \rho_B\right]. \tag{29}$$

As the pressure increases $\overline{P} - \Delta P \rightarrow \overline{P} + \Delta P$,

$$f_\uparrow(\overline{P} + p) = f(\overline{P} - \Delta P) + \int_{\overline{P}-\Delta P}^{\overline{P}+p} dP_c \int_{\overline{P}-\Delta P}^{P_c} dP_o \cdot \left[A(\overline{P} + p')\delta(P_c - P_o) + \rho_B\right]. \tag{30}$$

Thus

$$\frac{1}{K_\downarrow} = \Delta\epsilon\left[a_0 + a_1 p + a_2 \frac{p^2}{2} \cdots + (\Delta P - p)\rho_B\right], \tag{31}$$

and

$$\frac{1}{K_\uparrow} = \Delta\epsilon\left[a_0 + a_1 p + a_2 \frac{p^2}{2} \cdots + (\Delta P + p)\rho_B\right]. \tag{32}$$

The subscripts $\uparrow$ and $\downarrow$ indicate that the modulus is appropriate to pressure increase or decrease; p is the departure of the pressure from the ambient pressure $\overline{P}$. From Eqs. (31)–(32) we see that:

1. If $\rho_B = 0$ the modulus is a power series in p and $K_\uparrow$ is equivalent to $K_\downarrow$. This is essentially the traditional theory, sketched in Sec. II, where $p \propto \nabla \cdot \mathbf{u}$.
2. For $\rho_B \neq 0$ the elastic modulus is hysteretic, $K_\uparrow \neq K_\downarrow$.
3. For $\rho_B \neq 0$ the elastic modulus depends not only on the instantaneous value of the pressure but also on the amplitude of the pressure excursion.

Treating Eq. (25) systematically, we write

$$\rho_0 \frac{\partial^2 u}{\partial t^2} = \overline{K} \frac{\partial^2 u}{\partial x^2} + \frac{\partial}{\partial x}\left(\Delta K[u] \frac{\partial u}{\partial x}\right), \tag{33}$$

where

$$\overline{K} = \Delta\epsilon(a_0 + \rho_B \Delta P) \rightarrow \Delta\epsilon a_0 \tag{34}$$

is the dynamic modulus (the modulus as $\Delta P \rightarrow 0$). Keeping terms to first order in p

$$\Delta K = \Delta\epsilon \left[a_1 + \rho_B \text{sign}\left(\frac{\partial p}{\partial t}\right)\right] p. \tag{35}$$

The static modulus at ambient pressure $\overline{P}$ can be calculated in the same manor as the dynamic modulus. For the static modulus, as pressure increases f includes all of the mechanical elements in the vertical column, i.e.,

$$f_{\text{static}\uparrow} = \int_0^{\overline{P}} dP_c \int_0^{P_c} dP_o \;\; \rho(P_c, P_o). \tag{36}$$

Clearly $f_{\text{static}} \geq f_{\text{dynamic}}$ so that $K_{\text{dynamic}} \geq K_{\text{static}}$. This result follows from the behavior of $\rho(P_c, P_o)$. If there is hysteresis, there are mechanical elements that are not reversible and thus not on the diagonal in P-M space. The inequalities in f and K follow. This result was understood by Walsh (1965) and easily anticipated from the discussion given by Holcomb (1981). Using the PM space of Fig. 9 we can make predictions and comparisons of K_{static} and K_{dynamic} for this sample of Berea sandstone. We find that at $\overline{P} = 7.22$ MPa, the static moduli are $K_\uparrow = 10.0$ GPa and $K_\downarrow = 13.5$ GPa, while the dynamic modulus is $K_{\text{dynamic}} = 23.3$ GPa, a difference of a factor of two without resorting to any frequency dependent effects.

Wave propagation admitted by Eq. (25) can be described using the Green function formalism developed by McCall (1994). The first step in this formalism is to develop a systematic hierarchy of equations,

$$\frac{\partial^2 u_0(x,t)}{\partial t^2} - \overline{K} \frac{\partial^2 u_0(x,t)}{\partial x^2} = S(x,t), \tag{37}$$

$$\frac{\partial^2 u_1(x,t)}{\partial t^2} - \overline{K} \frac{\partial^2 u_1(x,t)}{\partial x^2} = \frac{\partial}{\partial x}\left(\Delta K[u_0] \frac{\partial u_0}{\partial x}\right), \tag{38}$$

where $u = u_0 + u_1 + \cdots$.

5.2 Longitudinal wave propagation

Suppose $S(x,t)$ in Eq. (37) causes a plane wave, $u_0 \propto U\cos(kx - \omega t)$. The first order correction to u_0 takes the form

$$u_1(x,\omega) = \int dx' G(x,x';\omega) \cdot \frac{\partial}{\partial x'}\left(\Delta K[u_0(x',\omega)] \frac{\partial u_0(x',\omega)}{\partial x'}\right). \tag{39}$$

From Eq. (35), $\Delta K \propto p \propto \partial u_0/\partial x$, thus $u_1 \propto (\partial u_0/\partial x)^2 \propto U^2$. Because of the discontinuity in ΔK, u_1 contains all harmonics of the fundamental, i.e., ω, 2ω, 3ω, ... This result is in contrast to the traditional theory in which each higher harmonic is associated with a higher power of u_0. Further development of Eqs. (33)–(35) and their consequences can be found in McCall (1994); McCall and Guyer (1994); Guyer et al. (1995).

5.3 Nonlinear attenuation

The hysteresis in a stress-strain measurement is often used to calculate energy loss. We define the quality factor Q by

$$\frac{1}{Q} = \frac{\Delta E}{\overline{E}}, \tag{40}$$

where ΔE is the energy loss per strain cycle and $\overline{E}$ is the average energy during a cycle. For ΔE we take

$$\Delta E = \frac{1}{\rho_0} \oint \sigma d\epsilon, \tag{41}$$

where $\oint$ stands for integration over one cycle in time, and σ is the effective stress in Eq. (33),

$$\sigma = (\overline{K} + \Delta K) \frac{\partial u}{\partial x}. \tag{42}$$

We develop ΔE as a series in the strength of the nonlinearity in direct analogy with the method of solution to Eq. (33) (McCall, 1994). To first order $\Delta E = \Delta E_0 + \Delta E_1$, where ΔE_0 is the contribution to the energy loss due to the linear elastic response of the system and

$$\Delta E_1 = \frac{1}{\rho_0} \oint \Delta K \frac{\partial u_0}{\partial x} \frac{\partial^2 u_0}{\partial x \partial t} dt. \tag{43}$$

Using $u_0 \propto U\cos(kx - \omega t)$, we have

$$\frac{\partial u_0}{\partial x} \frac{\partial^2 u_0}{\partial x \partial t} \propto -\frac{U^2 k^2 \omega}{2} \sin(2kx - 2\omega t). \tag{44}$$

The integral around a cycle in time picks out the term in ΔK that is proportional to $\sin(2kx - 2\omega t)$. The discontinuity in ΔK, resulting in all harmonics, leads to nonlinear attenuation. In the work of Day and Minster (1984), nonlinear attenuation Q is found to be the cause of hysteresis. Here, in contrast, we find hysteresis to be the cause of nonlinear attenuation.

5.4 Resonant bar experiments

In a resonant bar experiment an elastic system is driven at frequency ω and the amplitude of the response at the driving frequency is detected. At fixed amplitude of the drive A_D the frequency of the drive is swept through the resonance of the bar. The amplitude of the drive is stepped (increased) through a sequence of levels and the behavior of the frequency response at each drive level is measured. For a linear elastic material the bar

resonates at a frequency that is independent of the drive level. For a nonlinear elastic material the frequency response has a bent tuning-fork shape (Stoker, 1950). For a rock, this shape is that of a softening nonlinearity, i.e., the resonant frequency decreases with increasing drive amplitude.

Application of the traditional theory of nonlinear elasticity to the resonant bar experiment leads to simple predictions with verifiable signatures. Because the response of the bar is detected at the driving frequency the important nonlinearities are those that have contributions at the drive frequency. Above we argued that the cubic anharmonicity, A, B and C, generates $\omega + \omega = 2\omega$ and $\omega - \omega = 0$. Thus the most important term in the traditional theory of the resonant bar is the quartic nonlinearity (McCall and Guyer, 1994). The quartic nonlinearity leads to $\omega + \omega - \omega = \omega$ with amplitude proportional to the square of the drive level. Thus the traditional theory predicts a downward frequency shift,

$$\Delta\omega \propto A_D^2. \tag{45}$$

This result is well known for the soft Duffing oscillator (Stoker, 1950) and might be expected for rock, where a softening nonlinearity is found (Johnson and Rasolofosaon, 1996). However, the experimental frequency shift for rock is directly proportional to the drive level, $\Delta\omega \propto A_D$. Furthermore the order of magnitude of the observed frequency shift is orders of magnitude greater than that predicted by the traditional theory (using plausible values of the quartic nonlinearity).

Recently we have used Eq. (38) to describe the resonant bar experiment (Guyer et al., 1995). The most important point in the discussion is the form of the dynamic modulus. When a wave of pressure amplitude ΔP propagates in the system there is a secular change in the dynamic modulus $\overline{K}$ due to the term $\rho_B \Delta P$ in Eq. (34). This term in the modulus gives rise to a shift in the velocity of sound proportional to ΔP and thus to a shift in the resonance frequency proportional to $\Delta P \propto U$. Equation (34) can be made quantitative using the $\rho(P_c, P_o)$ for Berea sandstone from Guyer et al. (1995). A qualitative and quantitative description of the resonant bar experiment results.

6 Conclusion

In this paper we have given an overview of a comprehensive theory of the elastic behavior of consolidated materials. The discussion was given in terms of rocks; its generalization to other materials having the hysteresis and memory features similar to rock is straightforward. Some of our results were anticipated by others. Walsh (1965) recognized the significance of hysteresis in the static stress-strain equation of state and described the relationship between static and dynamic modulus. More recently Nazarov et al. (1988) gave a description of a resonant bar experiment using a modification of the five constant theory motivated by hysteresis in rock elastic behavior.

The elastic properties of homogeneous materials are accurately described by the five constant theory. Consolidated materials are different and are therefore of interest, i.e., it is the departure of the behavior of consolidated materials from that of homogeneous materials that causes one to give them special attention. We have sketched the outlines of a theoretical framework to describe the elastic properties of consolidated materials. This theoretical framework is much more complicated than the five-constant theory. In place of K, μ, A, B, and C we have introduced $\rho(P_c, P_o)$, the density in P-M space. Let us call the new theoretical framework the ρ theory. In the limit that $\rho_B \to 0$, Eqs. (18)–(19), ρ theory reduces to the five constant theory. Away from this limit the ρ theory predicts a variety of behaviors that have no explanation in the five constant theory: hysteresis, discrete memory, $K_{dynamic} \geq K_{static}$, nonlinear attenuation, copious higher harmonics, the outcome of a resonant bar experiment, etc.

We close with a series of observations about linear and nonlinear elasticity in rock.

1. The hysteretic mechanical elements with which we have developed the theory are very simple, only as complicated as the data requires. The mechanical elements at work in a consolidated material are much more complicated than this. More complicated models of the mechanical elements should be considered. More exhaustive σ-ϵ data sets will force the use of more elaborate mechanical elements. Eventually a detailed picture of the properties of the mechanical elements will be revealed.

2. The one dimensional model we have used is the result of an effective medium theory (McCall and Guyer, 1994). Within effective medium theory it is not possible to explain hysteresis in the elastic constant (Gist, 1994). McCall and Guyer (1994) have shown how hysteresis in the modulus can be found using a mean field theory. Ultimately it will be of interest to study the static and dynamic behavior of a lattice of hysteretic elements. Work to be undertaken in the future is the theoretical investigation of such systems.

3. One would expect the mechanical elements to respond to the pressure across themselves on a time scale set by their mechanics. Thus for each mechanical element there is a relaxation time that separates its low frequency response from its high frequency response. We have made no effort to incorporate such a time scale in this description. Should a suitable data set demand it, appropriate modification of the theory can be made.

4. Hysteretic mechanical elements imply attenuation. In addition to the nonlinear energy loss that occurs in the hysteretic mechanical elements there are attenuation mechanisms of the more traditional kind. For example, the squirt-flow mechanism. The squirt-flow mechanism and other linear attenuation mechanisms have been ignored in our presentation. They are easily added to the linear part of the basic wave equation as for example in McCall and Guyer (1994).

5. The inverse problem set by a modulus-strain data set is ill-posed. We have illustrated the result of one procedure (simulated annealing) for solving this problem. Experience may lead to the use of other inversion procedures.

6. The math/physics problem set by Eq. (25) has intrinsic interest. One can imagine a number of simple models generated by this problem. For example

$$\frac{\partial^2 u}{\partial t^2} + c_0^2 \left[1 - \beta + 2\beta\theta \left(\frac{\partial^2 u}{\partial x \partial t} \right) \right] \frac{\partial^2 u}{\partial x^2} = 0, \qquad (46)$$

where θ is the Heaviside function. This problem is similar to the kicked rotor.

Acknowledgements. The theory described here was developed in the context of dialogues with many of our colleagues, especially G. N. Boitnott, R. J. O'Connell, P. A. Johnson, A. Kadish and T. J. Shankland. This research is supported by the Office of Basic Energy Science, Engineering and Geoscience under contract W7405-ENG-36; the U. S. Department of Energy, Office of Arms Control and Nonproliferation under contract ST604; and the Institute for Geophysics and Planetary Physics at Los Alamos National Laboratory.

References

Ashcroft, N. W., and Mermin, N. D., *Solid State Physics*, Holt, Rinehart, and Winston, New York, 1976.

Boitnott, G. N., Fundamental observations concerning hysteresis in the deformation of intact and jointed rock with applications to nonlinear attenuation in the near source region, in Proceedings of the Numerical Modeling for Underground Nuclear Test Monitoring Symposium, *Los Alamos Natl. Lab. Rep., LA-UR-93-3839*, 121, 1993.

Bourbie, T., Coussy, O., and Zinszner, B. F., *Acoustics in Porous Media*, Gulf, Houston, 1987.

Cheng, C. H., and Toksöz, M. N., Inversion of seismic velocities for the pore aspect ratio spectrum of a rock, *J. Geophys. Res., 84*, 7533, 1979.

Day, S. M., and Minster, J. B., Numerical simulation of attenuated wavefields using a Pade approximant method, *Geophys. J. R. Astr. Soc., 78*, 105, 1984.

Gist, G. A., Fluid effects on velocity and attenuation in sandstones, *J. Acoust. Soc. Am., 96*, 1158, 1994.

Gol'dberg, Z. A., Interaction of plane longitudinal and transverse elastic waves, *Sov. Phys. Acoust., 6*, 306, 1960.

Guyer, R. A., McCall, K. R. and Boitnott, G. N., Hysteresis, discrete memory and nonlinear wave propagation in rock, *Phys. Rev. Lett., 74*, 3491, 1995.

Guyer, R. A., McCall, K. R., Johnson, P. A., Rasolofosaon, P. N. J., and Zinszner, B., Equation of state hysteresis and resonant bar measurements on rock, in *Proceedings of the 35th U. S. Rock Mechanics Sympopsium*, edited by J. J. K. Daemen and R. A. Schultz, Balkema, Rotterdam, 1995.

Hilbert, Jr., L. B., Hwong, T. K., Cook, N. G. W., Nihei, K. T., and Myer, L. R., Effects of strain amplitude on the static and dynamic nonlinear deformation of Berea sandstone, in *Rock Mechanics*, proceedings of the 1st North American Rock Mechanics Symposium, Austin, Texas, edited by P. P. Nelson and S. E. Laubach, Balkema, Rotterdam, 1994.

Holcomb, D. J., Memory, relaxation, and microfracturing in dilatant rock, *J. Geophys. Res., 86*, 6235, 1981.

Ilinskii, Y. A., and Zabolotskaya, E. A., Cooperative radiation and scattering of acoustic waves by gas bubbles in liquids, *J. Acoust. Soc. Am., 92*, 2837, 1992.

Johnson, D. L., Kostek, S., and Norris, A. N., Nonlinear tube waves, *J. Acoust. Soc. Am., 96*, 1829, 1994.

Johnson, P. A., and McCall, K. R., Observation and implication of nonlinear elastic wave behavior in sandstone, *Geophys. Res. Lett., 21*, 165, 1994.

Johnson, P. A., and Rasolofosaon, P. N. J., Nonlinear elasticity and stress-induced anisotropy in rocks - reflections on experimental results, Proceedings of the Soc. Exp. Geophys. 63rd Annual Meeting, 1993.

Johnson, P. A., and Rasolofosaon, P. N. J., Manifestation of nonlinear elasticity in rock: convincing evidence over large frequency and strain intervals from laboratory studies, in this volume, 1996.

Jones, L. J., and Kobett, D. R., Interaction of elastic waves in an isotropic solid, *J. Acoust. Soc. Am., 35*, 5, 1963.

Landau, L. D., and Lifshitz, E. M., *Theory of Elasticity*, Pergamon, New York, 1959.

Mayergoyz, J. D., Hysteresis models from the mathematical and control theory points of view, *J. Appl. Phys., 57*, 3803, 1985.

McCall, K. R., Theoretical study of nonlinear elastic wave propagation, *J. Geophys. Res., 99*, 2591, 1994.

McCall, K. R., and Guyer, R. A., Equation of state and wave propagation in hysteretic nonlinear elastic materials, *J. Geophys. Res., 99*, 23887, 1994.

Meegan, Jr., G. D., Jr., Johnson, P. A., Guyer, R. A., and McCall, K. R., Observations of nonlinear elastic wave behavior in sandstone, *J. Acoust. Soc. Am., 94*, 3387, 1993.

Murnaghan, F. D., *Finite Deformation of an Elastic Solid*, John Wiley, New York, 1951.

Nazarov, V. E., Ostrovsky, L. A., Soustova, I. A., and Soutin, A. M., Nonlinear acoustics of micro-inhomogeneous media, *Phys. Earth Planet. Inter., 50*, 65, 1988.

O'Connell, R. J., and Budiansky, B., Measures of dissipation in viscoelastic media, *Geophys. Res. Lett., 5*, 5, 1978.

Preisach, F., Über die magnetische Nachwirkung, *Z. Phys., 94*, 277, 1935.

Press, W. H., Flannery, B. P., Teukolsky, S. A., and Vetterling, W. T., *Numerical Recipes: The Art of Scientific Computing*, Cambridge, New York, 1986.

Scholz, C. H. and Hickman, S. H., Hysteresis in the closure of nominally flat joints, *J. Geophys. Res., 88*, 6501, 1983.

Stoker, J. J., *Nonlinear Vibrations in Mechanical and Electrical Systems*, Interscience, New York, 1950.

Walsh, J. B., The effect of cracks on the uniaxial elastic compression of rocks, *J. Geophys. Res., 70*, 399, 1965.